Supporting Information

Yang et al. 10.1073/pnas.1309629110

SI Materials and Methods

Animals. Male WT C57Bl6 and immunodeficient SCID mice at the age of 6 to 8 wk were used in this study and were obtained from the breeding unit at the Department of Microbiology, Tumor and Cell Biology at Karolinska Institute.

Cell Culture. T241 fibrosarcoma and Lewis lung carcinoma (LLC) cell lines that stably expressed placental growth factor-1 (PlGF-1) or an empty vector were generated as previously described (1–3). VEGF-null fibrosarcoma tumor cell line (528ras1) was provided by Janusz Rak (McMaster University, Hamilton, ON, Canada). All transfected and nontransfected tumor cells were grown and maintained in DMEM (cat. no. SH30243.01; HyClone) supplemented with 10% (vol/vol) heat-inactivated FBS (cat. no. SH30160.03; HyClone).

Antibodies. Antibodies used in this study included a rat anti-mouse CD31 antibody (cat. no. 553370; 1:200 dilution; BD Pharmingen), a goat anti-mouse CD31 (cat. no. AF3628; 1:200 dilution; R&D Systems) antibody, a rabbit anti-mouse NG2 (cat. no. AB5320; 1:200 dilution; Millipore) antibody, a mouse anti-human α-SMA (clone 1A4; 1:200 dilution; Dako) antibody, an Alexa Fluor-555–conjugated goat anti-rat antibody (cat. no. A21434; 1:200 dilution; Invitrogen), a Cy5-conjugated goat anti-rat antibody (cat. no. AP183S; 1:200 dilution; Chemicon), a Cy3-conjugated donkey anti-goat antibody (cat. no. LV1370387; 1:200 dilution; Jackson ImmunoResearch), a Cy5-conjugated goat anti-rabbit antibody (cat. no. AP132S; 1:200 dilution; Chemicon), and an Alexa Fluor-647–conjugated rabbit anti-mouse antibody (cat. no. A21239; 1:200 dilution; Invitrogen). An anti-mouse VEGF neutralizing antibody (ref. BD0801) was provided by Simcere Pharmaceutical and was used as previously described (3), and an anti-mouse VEGFR2 (DC101) neutralizing antibody (2–4) was prepared from a hybridoma cell line (American Type Culture Collection HB-11534).

Cell Proliferation Assay. In vitro cell proliferation was performed using a 3-(4,5-dimethylthiazol-2-yl)-2,5-diphenyltetrazolium bromide (MTT; cat. no. M5655; Sigma-Aldrich) assay as previously described (5). A total of 1,000 cells in 200 μL DMEM–10% (vol/vol) FBS were seeded into each well of 96-well plates. Cell proliferation was measured every 24 h by adding 20 μL MTT (5 mg/mL; cat. no. M5655; Sigma-Aldrich) to each well, followed by further incubation for 3 h, and measurement of absorbance at a wavelength of 490 nm of the purple formazan dissolved in 150 μL per well DMSO ($n = 6$ samples per group per day).

Mouse Tumor Experiments. Tumor cells were s.c. implanted into the middorsal region of each mouse ($n = 6$–8 mice per group). tumor sizes were measured every other day, and tumor-bearing mice were randomly divided into various groups to receive anti-VEGF or vehicle treatment. Approximately 1×10^6 tumor cells in 100 μL PBS solution were implanted s.c. into the middorsal region of each C57Bl6 or SCID mouse ($n = 6$–8 mice per group). Before tumor cell implantation, mice were anesthetized by inhalation of isoflurane (Abbott Scandinavia). tumor sizes were measured every other day, and tumor sizes were calculated according to a standard formula as previously described (6, 7). In some experiments, tumor-bearing mice were randomly divided into various groups to receive anti-VEGF or vehicle treatment. VEGFR2 blockade at a dose of 400 μg per mouse and VEGF blockade at a dose of 50 μg per mouse was injected i.p. into each mouse every 4 d starting on day 1. At the end of experimentation, mice were euthanized, and tumor tissues were immediately fixed with 4% (wt/vol) paraformaldehyde (PFA) at 4 °C overnight. For the vascular permeability and perfusion assay, 100 μL lysine-fixable tetramethylrhodamine 70 kDa (cat. no. D1818; Invitrogen) dextran or 2,000 kDa dextran (cat. no. D7139; Invitrogen) was injected into the tail vein of each tumor-bearing mouse at the end of experiment, mice were euthanized 15 min or 5 min after injection, and the tumor tissues were immediately fixed with 4% (wt/vol) PFA at 4 °C overnight.

Whole-Mount Staining. Tissue whole-mount staining was performed according to our previously described method (8–12). Stained tissues were mounted in a Vectashield mounting medium (cat. no. H-1000; Vector Laboratories) and stored at −20 °C in darkness until examination under a confocal microscope (LSM510 confocal microscope; Zeiss). For 3D image analysis, consecutive scanning of six layers were assembled to constitute one dataset by using a confocal microscope software program (EZ-C1). Quantitative analyses were performed from at least 24 different random areas by using Adobe Photoshop CS software.

Quantitative Real-Time PCR. Fresh vector and PlGF-expressing VEGF-null tumors were used for total RNA isolation. Total RNA isolated from vector and PlGF-expressing VEGF-null tumors was used for quantitative PCR (qPCR) analysis. Total RNA (2 μg) from each sample was reverse-transcribed by using a RevertAid H minus First Strand cDNA Synthesis Kit (Fermentas). Reverse-transcribed cDNA samples were directly subjected to qPCR using an ABI Prism 7,500 System (Applied Biosystems). Each PCR sample was performed in triplicates, and each reaction contained SYBR Green (Applied Biosystems), 150 nM forward and reverse primers, and 1 μL of cDNA. PCR was run for 40 cycles, and each cycle consisted of denaturation at 95 °C for 15 s, annealing at 60 °C for 1 min, and extension at 72 °C for 1 min. In the initial cycle, samples were incubated at 50 °C for 2 min and 94 °C for 10 min. The sequences of primer pairs were as follows: mouse *gapdh* forward 5′-CCAGCAAGGACACTGAGCAA-3′ and mouse *gapdh* reverse 5′-GGGATGGAAATTGTGAGGGA-3′; and mouse *vegfa* forward 5′-ATGAACTTTCTGCTCTCTTGGGT-3′ and mouse *vegfa* reverse 5′-ACACAGGACGGCTTGAAGATGTA-3′. The housekeeping gene *gapdh* was used as an internal control. The calculated *vegf* Ct value was normalized to the Ct value for *gapdh*, and the relative amount of transcripts was calculated by using the $2^{-\Delta\Delta}$Ct method as described previously (7). These values were then used for calculation of mRNA expression levels.

ELISA. Mouse VEGF and human PlGF were detected by using commercially available VEGF and PlGF ELISA kits (R&D Systems). The ELISA protocol was performed according to the manufacturer's instructions. Each ELISA experiment was acutely calibrated with standard amounts of known proteins as internal controls, and a linear concentration-dependent curve was established. Mouse VEGF/human PlGF (hPlGF) heterodimers were measured by using a sandwich method (3): an anti-mouse VEGF antibody at the concentration of 10 μg/mL in 100 μL PBS solution was added to each well of a 96-well plate, coated overnight at room temperature. Plates were thoroughly washed with a rinsing buffer containing 0.05% (vol/vol) Tween-20 in PBS (PBST), followed by blocking with 1% BSA (mass/vol) in PBS solution at room temperature for 1.5 h. Forty-eight–hour cultured tumor

cell-conditioned medium in 100 μL and a tumor cell lysate solution each containing 100 μg/mL protein were added to each well of a 96-well plate after various dilutions. Commercially available VEGF-PlGF heterodimers (R&D Systems) were used as a standard to calibrate concentration-dependent measurement. The reaction was incubated at room temperature for 2 h, followed by thoroughly washing with PBST. A biotinylated goat anti-human PlGF antibody (R&D Systems) was used as the detection antibody. Color development of ELISA-positive signals was performed according to the manufacturer's instruction. Triplicates of samples were used, and the experiments were repeated three times.

Statistical Analysis. Experimental data were analyzed by using a two-tailed Student t test. Statistical P values were as follows: $P < 0.05$ was significant, $P < 0.01$ was highly significant, and $P < 0.001$ was extremely significant. Data are presented as mean ± SEM.

1. Eriksson A, et al. (2002) Placenta growth factor-1 antagonizes VEGF-induced angiogenesis and tumor growth by the formation of functionally inactive PlGF-1/VEGF heterodimers. *Cancer Cell* 1(1):99–108.
2. Hedlund EM, Hosaka K, Zhong Z, Cao R, Cao Y (2009) Malignant cell-derived PlGF promotes normalization and remodeling of the tumor vasculature. *Proc Natl Acad Sci USA* 106(41):17505–17510.
3. Hedlund EM, et al. (2013) Tumor cell-derived placental growth factor sensitizes antiangiogenic and antitumor effects of anti-VEGF drugs. *Proc Natl Acad Sci USA* 110(2):654–659.
4. Cao R, et al. (2010) VEGFR1-mediated pericyte ablation links VEGF and PlGF to cancer-associated retinopathy. *Proc Natl Acad Sci USA* 107(2):856–861.
5. Cao R, et al. (2012) Collaborative interplay between FGF-2 and VEGF-C promotes lymphangiogenesis and metastasis. *Proc Natl Acad Sci USA* 109(39):15894–15899.
6. Zhang D, et al. (2011) Antiangiogenic agents significantly improve survival in tumor-bearing mice by increasing tolerance to chemotherapy-induced toxicity. *Proc Natl Acad Sci USA* 108(10):4117–4122.
7. Xue Y, et al. (2012) PDGF-BB modulates hematopoiesis and tumor angiogenesis by inducing erythropoietin production in stromal cells. *Nat Med* 18(1):100–110.
8. Jensen LD, et al. (2012) Opposing effects of circadian clock genes bmal1 and period2 in regulation of VEGF-dependent angiogenesis in developing zebrafish. *Cell Rep* 2(2): 231–241.
9. Cao Z, et al. (2010) Hypoxia-induced retinopathy model in adult zebrafish. *Nat Protoc* 5(12):1903–1910.
10. Lim S, et al. (2012) Cold-induced activation of brown adipose tissue and adipose angiogenesis in mice. *Nat Protoc* 7(3):606–615.
11. Cao R, et al. (2011) Mouse corneal lymphangiogenesis model. *Nat Protoc* 6(6): 817–826.
12. Xue Y, Lim S, Bråkenhielm E, Cao Y (2010) Adipose angiogenesis: quantitative methods to study microvessel growth, regression and remodeling in vivo. *Nat Protoc* 5(5):912–920.

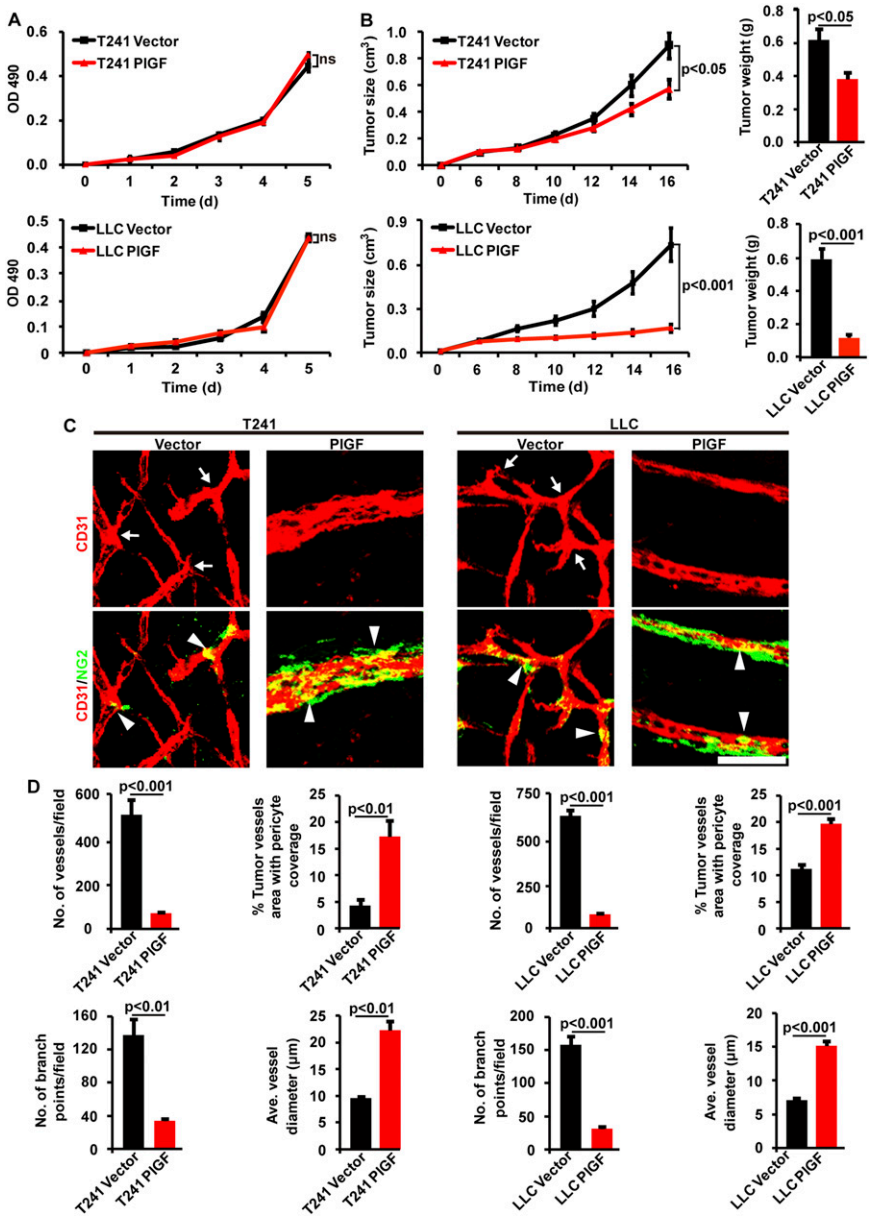

Fig. S1. PlGF in modulation of tumor growth, angiogenesis, and vascular remodeling (with the same T241 group as Fig. 1 to compare). (*A*) PlGF-overexpressing T241 fibrosarcoma and LLC carcinoma cell proliferation ($n = 6$ samples per group). T241 and LLC vector tumor cells served as controls ($n = 6$ samples per group; ns, not significant). (*B*) Tumor growth rates and weights in syngeneic C57bl6 mice ($n = 8$–10 mice per group). (*C*) Confocal images of $CD31^+$ tumor vessels (red; arrows) and $NG2^+$ pericyte coverage (green). Arrowheads point to vessel-associated pericytes. (Scale bar: 50 μm.) (*D*) Quantification of vessel numbers, pericyte coverage, numbers of vascular branching points, and vascular diameter in various tumors ($n = 24$ randomized fields per group).

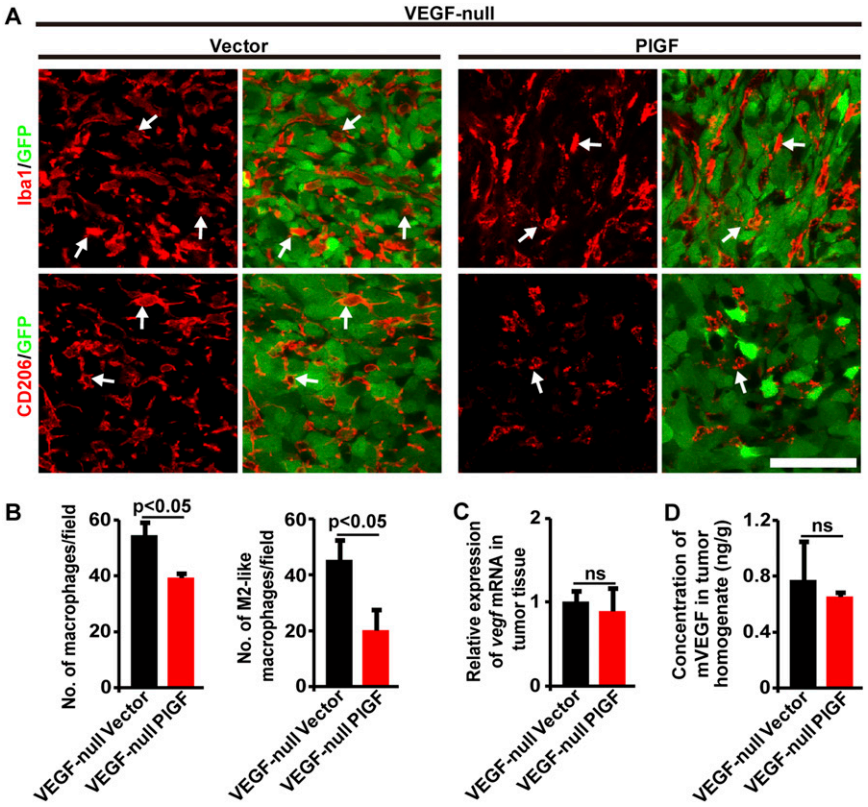

Fig. S2. Macrophages and tumor-associated macrophages in tumors. (*A*) Total numbers of macrophages in vector- and PlGF-expressing VEGF-null tumor tissues were detected by using Iba1 as a pan marker (red) and $EGFP^+$ tumor cell are shown in green. The M2 subpopulation macrophages were detected by using CD206 as a marker (red). Arrows point to macrophages in tumor tissues. (Scale bar: 50 μm.) (*B*) Quantification of total numbers of and $M2^+$ microphages in tumor tissues (n = 24–30 randomized fields per group; ns, not significant). (*C*) Quantification of VEGF mRNA levels in vector- and PlGF-expressing tumor tissues by qPCR (n = 3 different tumor tissues per group). (*D*) Quantification of VEGF protein levels in vector- and PlGF-expressing tumor tissues by ELISA (n = 3 different tumor tissues per group).

Table S1. Measurement of various dimeric VEGF and PlGF

Cell	hPlGF/hPlGF, ng/mL	mVEGF/mVEGF, ng/mL	hPlGF/mVEGF, ng/mL
Conditioned medium			
VEGF-null vector	ND	ND	ND
VEGF-null PlGF	28.914 ± 0.417	ND	ND
T241 vector	ND	0.949 ± 0.095	ND
T241 PlGF	12.694 ± 1.624	0.332 ± 0.021	14.708 ± 0.739
LLC vector	ND	0.886 ± 0.039	ND
LLC PlGF	9.280 ± 0.537	0.429 ± 0.035	5.332 ± 0.956
Cell lysate			
VEGF-null vector	ND	ND	ND
VEGF-null PlGF	0.789 ± 0.026	ND	ND
T241 vector	ND	0.147 ± 0.004	ND
T241 PlGF	0.511 ± 0.030	0.127 ± 0.004	0.773 ± 0.280
LLC vector	ND	0.609 ± 0.032	ND
LLC PlGF	2.253 ± 0.534	0.154 ± 0.013	3.914 ± 0.478

Data presented as mean ± SEM. hPlGF, human PlGF; mVEGF, mouse VEGF; ND, not detectable.